Millennial-scale changes in sea-surface temperature and productivity along the Kuroshio–Oyashio boundary during MIS-19 based on the radiolarian record from the Chiba composite section, central Japan

Takuya Itaki (t-itaki@aist.go.jp)
Geological Survey of Japan, AIST https://orcid.org/0000-0001-5232-0055
Sakura Utsuki
Chiba University
Yuki Haneda
Geological Survey of Japan
Kentaro Izumi
Chiba University
Yoshimi Kubota
National Museum of Nature and Science
Yusuke Suganuma
National Institute of Polar Research
Makoto Okada
Ibaraki University

Research article

Keywords: Paleoceanography, Lower-Middle Pleistocene GSSP, Interglacial, MIS-19, sea-surface temperature, teleconnection

Posted Date: April 29th, 2020

DOI: https://doi.org/10.21203/rs.3.rs-24663/v1

Abstract

A high-resolution radiolarian record from 800 to 750 ka was examined from the Chiba composite section (CbCS) of the Kokumoto Formation, including the GSSP (Global Boundary Stratotype Section and Point) for the Lower–Middle Pleistocene boundary, on the Boso Peninsula, Pacific side of central Japan. Total radiolarian abundance was closely related to biological productivity in the surface layer and was observed to increase and repeatedly decrease in the millennial-scale period. Summer SST (sea-surface temperature), which was estimated based on the radiolarian assemblage, was 19°C at the end of MIS-20 (790-793 ka) and fluctuated between 21 and 26°C during MIS-19, with the warm periods tending to be synchronous with high productivity. Recent observations have revealed that productivity increases with a northward shift of the Kuroshio along the Kuroshio-Oyashio boundary zone. Therefore, high productivity in the warmer and stratified conditions during MIS-19 can be interpreted as being closely related to millennial-scale oscillations of the Kuroshio Extension. Such millennial-scale climatic changes were also recognized in southern Europe and are likely related to shifts in climate systems such as AO (Arctic Oscillations) and PDO (Pacific Decadal Oscillations).

Introduction

Because Marine Isotope Stage (MIS)-19 is an interglacial period with an orbital composition of the Milankovitch cycle similar to that of the current interglacial (MIS-1), it is important to build a detailed understanding of the climatic features of this period for use in making future predictions (Tzedakis et al., 2012; Giaccio et al., 2015; Sánchez Goñi et al., 2016). The Kazusa Group composed of Pleistocene deep-sea deposition is continuously distributed on the Boso Peninsula on the Pacific side of central Japan (e.g., Kazaoka et al., 2015). Furthermore, the Chiba composite section (CbCS) of the Kokumoto Formation in this group is a well-exposed and continuous marine sedimentary record across MIS-19 (Fig. 1), which has been investigated in great detail from various aspects (GSSP Proposal Group, 2019; Suganuma et al., 2015; Nishida et al., 2015; Okada et al., 2017; Simon et al., 2019; Haneda et al., 2020; Haneda et al., submitted; Izumi et al., submitted; Kameo et al., submitted). Therefore, the CbCS was ratified as a GSSP (Global Boundary Stratotype Section and Point) for the Lower–Middle Pleistocene boundary.

At present, the offshore area near the Boso Peninsula is influenced by both the Kuroshio warm and Oyashio cold currents and, therefore, it is expected to be sensitive to the glacial-interglacial cycle and even small climatic changes in East Asia. Suganuma et al. (2018) discussed the close relationship between climatic changes in this area and climatic dynamics in East Asia based on the results of various proxies from the CbCS. Recently, more detailed millennial-scale studies from this section have been conducted for oxygen isotopes of foraminifera (Haneda et al., 2020), the geochemical record (Izumi et al., submitted) and calcareous nanofossils (Kameo et al., submitted).

Radiolarians, a marine plankton group with opaline skeletons, are preserved in deep-sea sediments as microfossils and are widely used as a paleoceanographic proxy. Examination of this microfossil group is well suited for detecting changes in the Kuroshio-Oyashio front that are closely related to past climatic

changes around the Boso Peninsula (e.g., Chinzei et al., 1987; Yasudomi et al., 2014). In total, 36 radiolarian species and species groups have been reported from the CbCS (Motoyama et al., 2017), and radiolarian assemblages related to climatic changes were reported in Suganuma et al. (2018) but with low-resolution, preliminary results, owing to the inclusion of few species.

In this study, we conducted high resolution analysis of radiolarian fossils during MIS-19 from the CbCS. Because radiolarians are secondary producers in the ecosystem, total abundance of the fossil serves as a proxy for biological productivity. In addition, sea-surface temperature (SST) in the past can be extrapolated from the faunal assemblage. In this paper, millennial-scale changes of paleoceanographic conditions during MIS-19 are discussed based on the results of this study and other proxies.

Methods

A total of 236 samples, including 195 new samples and 41 samples that were used for preliminary analysis in Suganuma et al. (2018), were processed for radiolarian analysis in this study (Supplementary Tables 1 and 2). Sampling locations, stratigraphic framework and age models are based on Suganuma et al. (2018) and Haneda et al. (2020) (Supplementary Fig. 1).

Freeze-dried samples were weighed and wet sieved using 45 μm meshes, and then two types of slides were prepared for quantifying the abundance (Q-slide) and for faunal analysis (F-slide) based on the standard technique described in Itaki et al. (2018). The total number (abundance) of radiolarians in 1 g of dry sediment was estimated using the following equation:

Total radiolarian abundance (individuals/g)

= total number of individuals on Q-slide x 200 / sample weight (g)

For the 195 samples newly collected in this study, the relative abundance (% of total assemblage) of the species was estimated by counting and identifying more than 300 individuals on the F-slide; however, when radiolarian individuals were scarce, as many as could be identified were counted (Supplementary Table 1). Radiolarians were observed under an optical microscope at x40 to x200 magnification. Identifications were made using a taxonomic framework adapted from Itaki (2009) and Matsuzaki and Itaki (2017).

Matsuzaki and Itaki (2017) proposed a radiolarian-based transfer function equation for the estimation of summer SST from surface sediments in the northwestern Pacific. However, it is difficult to perform accurate reconstruction using this equation for results from the CbCS due to the restriction of taxonomic categories for counting. Therefore, Suganuma et al. (2018) applied the Tr value to preliminary results from the CbCS. The Tr value is a radiolarian-based climate index originally proposed by Nigrini (1970) that has the following simple equation using only limited indicator species:

$Tr = Xw / (Xw + Xt + Xc)$

where Xw, Xt and Xc are the number of warm-, temperate and cold-water radiolarian species and species groups, respectively, and data used to estimate Tr values in this study are listed in Supplementary Table 2.

Furthermore, looking at the radiolarian data of Matsuzaki and Itaki (2017), which was compiled using the same radiolarian analysis method as in this study, we can see a correlation between Tr values and summer SST with r = 0.97 (Fig. 2). The following binomial equation derived from this relationship was applied to the CbCS results to estimate the paleo SST.

Summer SST (°C) = $-13.9 \times Tr^2 + 22.2 \times Tr + 13.1$

Results And Discussion

Total radiolarian abundance

Radiolarian fossils were collected from all analyzed samples but had poor to moderate levels of preservation. Total radiolarian abundance ranged between 80 to 1,300 individuals/g with higher values during the peak of MIS-19c as reported in Suganuma et al. (2018). Further, periodic fluctuations with about 2,000 to 3,000 year intervals were observed during the study period.

Generally, changes in the number of radiolarians that are secondary producers are closely related to primary production at the near sea-surface and can therefore be used as an indicator of relative productivity. In Fig. 3, TOC (total organic carbon) and Ca/Ti (calcium/titanium ratio), which are indicators of productivity obtained from the CbCS (Izumi et al., submitted), show a general tendency to increase with radiolarians in MIS-19.

In addition, some of the short-cycle fluctuations observed in radiolarians also show synchronized changes, but there are also periods of non-synchronization. Ca/Ti shows a peak value at 771 to 787 ka, and short-period fluctuations observed in radiolarians are not confirmed. Ca/Ti is associated with an increase or decrease in shells of foraminifera and coccolith with carbonate skeletons, while radiolarians of secondary producers reflect overall biological production, including other producers. Therefore, short-period fluctuations not recorded in carbonate would have been recorded in radiolarians. TOC, like radiolarian, reflects overall biological production. In fact, many short cycle variations appear to be synchronous with those of radiolarians. However, TOC maxima at 760 and 764 ka did not coincide with radiolarian peaks. According to Izumi et al. (submitted), these fluctuations are interpreted as being due to oxygen-depleted bottom-water conditions. That is, oxygen consumed due to stagnation of the water mass improved the preservation of organic matter near the bottom. For these reasons, total changes in radiolarian abundance are considered to be more effective for estimating relative primary productivity in the sea.

Radiolarian assemblages

In this high-resolution analysis, a total of 30 species and species groups were counted (Supplementary Table 1). *Tetrapyle circularis* Müller group, *Spongodiscus resurgens* Ehrenberg, *Larcopyle buetchlii* Dreyer, *Stylodictya* spp., *Didmocyrtis* spp. and *Lithomelissa setosa* Jørgensen were predominant, and *Ditctyocoryne* spp., *Stylochlamydium venustum* Bailey, *Amphirhopalum ypsilon* Haeckel, *Druppatractus irregularis* Popofsky, *Euchitonia* spp., *Lithelius minor* Jørgensen and *Cycladophora davisiana* Ehrenberg were also observed.

Among the species, *T. circularis* group, *Didmocyrtis* spp., *Ditctyocoryne* spp., *A. ypsilon* and *Euchitonia* spp. are subtropical species characteristic of the Kuroshio region according to Matsuzaki and Itaki (2017), and these accounted for 5–45% of the radiolarian assemblage in the CbCS. At present, higher abundances of these groups occur in the Kuroshio Current where sea-surface temperatures range between 20 and 29 °C (Matsuzaki and Itaki, 2017). On the other hand, *S. resurgens*, *L. setosa*a and *S. venustum* characterize the cold-water mass of the Oyashio region, accounting for 7–37% of radiolarians in the CbCS. These groups are associated with cold waters ranging from 12 to 18 °C (Matsuzaki and Itaki, 2017). While warm-water species increased during MIS-19, cold-water species tended to increase in MIS-20 and MIS-18. The temperate species *L. buetschlii* shows variation similar to the cold-water assemblage. *Larcopyle minor* and *Cycladophora davisiana* are both deep dwellers adapted to middle and high latitudes in the North Pacific, respectively (Matsuzaki and Itaki, 2017).

SST reconstruction

The Tr value was estimated using the indicator species shown in Supplementary Table 2 and Supplementary Fig. 2, which were found in common in this study and in Suganuma et al. (2018). The Tr value fluctuated considerably between 0.2 and 0.8 throughout the examined period, and the multiple maxima and minima likely reflect oscillations of the Kuroshio Current. Figure 3 shows summer SST variations in the CbCS converted from the Tr value. The water temperature varied from 16 to 27° C, and the lowest SST was observed at the end of MIS-20 (790–794 ka). This pattern is generally consistent with results from the oxygen isotope ratio of planktonic foraminifera *Globigerina bulloides* d'Orbigny ($\delta^{18}O_{Gb}$), except for during MIS-19c. Minor inconsistencies between summer SST and $\delta^{18}O_{Gb}$ during MIS-19c might be due to differences in the season in which these data were recorded; radiolarian-based SST is estimated as summer values, while it is expected that $\delta^{18}O_{Gb}$ is largely determined in spring based on the modern production season of *G. bulloides* reported from sediment trap experiments in the northwestern Pacific Ocean (Kuroyanagi et al., 2002).

Distinct millennial-scale fluctuations ranging between 20 and 27 °C were observed during MIS-19. This variation is almost synchronized with the oxygen isotope ratio of the surface species of planktonic foraminifera (Fig. 3). The current summer SST near the Boso Peninsula is around 26 °C, which almost corresponds to the highest value of the reconstructed temperature. On the other hand, the temperature was 20 to 24 °C in cold periods of MIS-19, which corresponds to the current Fukushima-Sendai offshore. That is, most of MIS-19 was 2 to 6 °C cooler than the present, suggesting the strong influence of the Oyashio Current. Tanaka et al. (2017) reported that the annual SST ranged between 16 and 23 °C during

MIS-19 based on diatom fossil assemblages from core TB2, which was drilled near the CbCS. They noted that the SST shifted from the Oyashio phase to the Kuroshio phase at 770 ka; however, such a trend in the climatic shift was not observed in our record.

Millennial-scale Kuroshio fluctuations during the interglacial state have also been reported from other interglacial periods. Holocene 1500-year cycles of the SST fluctuations have been reported based on UK^{37} (Isono et al., 2009) and diatom fossil assemblages (Koizumi, 2008) from a marine sedimentary core (MD01-2421), which were collected from the western Pacific at 36°N near the Boso Peninsula. In their studies, the amplitude of water temperature fluctuation was estimated to be about 1 °C. Yasudomi et al. (2014), who examined in detail the radiolarians of the last interglacial period (MIS-5e) using the same core, showed that the Tr value fluctuated with a 500-year cycle. The Tr value (0.6–0.9) in their study corresponded to a range of 26 to 28 °C according to the summer SST derived from the equation in this study. Thus, the water temperature in the Holocene and MIS-5e was higher and had a smaller fluctuation than in MIS-19.

The slightly colder oceanic paleotemperature condition during MIS-19 is consistent with the larger temperature amplitudes of the millennial-scale fluctuations because the latitude gradient in temperature is larger in this zone. The slightly colder oceanic conditions are also consistent with lower temperatures revealed by regional vegetation records in the CbCS (Suganuma et al., 2018). Such a zonal shift in the climatic zone is reasonably explained by lower atmospheric CO_2 concentration during MIS-19 (Bereiter et al., 2015).

Relationship between productivity and SST

The millennium-scale productivity maxima inferred from the total radiolarian abundance tends to be during the warmer and cooler intervals that appeared after and before 785 ka, respectively (Fig. 3). The high productivity observed during cooler intervals observed at the end of MIS-20 and the earliest part of MIS-19 is likely affected by the high nutrient supply from the Oyashio water with a southward shift of the polar front (Fig. 4c), which is probably a response to the southward shift of the westerly jet with intensification of the winter Aleutian Low, as discussed by Suganuma et al. (2018) and Haneda et al. (2020). On the other hand, high productivity during warmer intervals during MIS-19 can be explained by decadal observations of modern oceanic conditions. Nishibe et al. (2015) proposed that high productivity is caused by development of favorable photosynthesis conditions with a layered structure, in which the high temperature Kuroshio water overlays the low temperature Oyashio water. In addition, the areal extent of the Kuroshio-Oyashio layered structure varies from year-to-year, and this interannual variability affects primary productivity, making it possible to relate these variations to inter-decadal climate regime shifts in the North Pacific (Nishikawa et al., 2016) such as the PDO (Pacific Decadal Oscillation) (e.g., Minobe, 2002). Therefore, increases in productivity during warmer phases are periodically recognized during MIS-19 in the CbCS and are likely the result of the expansion and retreat of layered structures (Fig. 4a, b).

The millennial-scale climatic changes during MIS-19 can also be recognized in records from the northern Atlantic Ocean (Kleiven et al., 2011) and central Europe (Giaccio et al., 2015; Sánchez Goñi et al., 2016;

Regattieri et al., 2019). Figure 5 shows the probable correlations between climate records for the Sulmona Basin in Italy (Giaccio et al., 2015; Regattieri et al., 2019) and the CbCS in Japan (this study). Synchronous trends in each region suggest the strength of a large-scale teleconnection over the northern hemisphere of the Arctic Oscillation (AO) associated with winter Aleutian Low intensity (Tompson and Wallace, 1998) during MIS-19. The wet conditions in southern Europe were caused by the southern shift of westerly storm tracks during the negative phase of the AO. On the other hand, the Kuroshio transport increased with the intensification of the Aleutian Low during the negative AO (Deser et al., 1999). As shown in Fig. 5, a consistent relationship is seen between paleo-records of humidity in southern Italy and the Kuroshio expansion in the CbCS during MIS-19.

Conclusions

High resolution radiolarian analysis for the MIS-19 period was performed on the Chiba composite section, including the Lower-Middle Pleistocene GSSP, and paleoceanographic changes were compared with geochemical proxies reported from the same section.

The total radiolarian abundance showed millennial-scale variations with a tendency for synchronized TOC and Ca/Ti, which is an effective proxy of productivity.

Surface water temperature records reconstructed from the assemblages varied between 19 and 26 °C and tended to be synchronized with planktonic oxygen isotope records. The Younger Dryas-like event at the end of MIS-20 showed the lowest value, and millennia-scale fluctuations ranging between 21 and 26 °C were observed during MIS-19. SST during MIS-19 seems to have been slightly colder than during other interglacial periods such as the Holocene and MIS-5e.

High productivity with millennial-scale periodicity during MIS-19 tended to increase with the development of the layered Kuroshio-Oyashio structure during warm periods. This is likely related to expansion of favorable conditions for photosynthesis, such as the light environment, with the overlay of the warm Kuroshio water on the cold Oyashio water.

Millennial-scale fluctuations in the surface water temperature during MIS-19 can be correlated with European climate changes (Giaccio et al., 2015; Sánchez Goñi et al., 2016; Regattieri et al., 2019), and these are thought to have emerged as a result of atmospheric circulation teleconnection over a wide area. However, there are limited reports of high-resolution analysis in MIS-19, and it is expected that detailed teleconnection mechanisms will be elucidated by comparing analysis results over wide geographic areas.

Abbreviations

AO
Arctic Oscillations
Ca/Ti
Calcium/titanium ratio

CbCS
Chiba composite section
GSSP
Global Boundary Stratotype Section and Point
M–B boundary
Matuyama–Brunhes boundary
MIS
Marine Isotope Stage
PDO
Pacific Decadal Oscillations
SST
Sea-surface temperature
TOC
Total organic carbon
$\delta^{18}O$
Oxygen isotope ratio

Declarations

Availability of data and material

The datasets supporting the conclusions of this paper are available as additional files (Supplementary Table 1).

Competing interests

The authors declare that they have no competing interests.

Funding

This work was supported by JSPS KAKENHI Grant numbers 16H04068 and 19H00710 (MO).

Authors' contributions

TI conceived of the experiments and wrote the manuscript. TI and SU conducted the experiments. YH, KI and YK contributed to determining geochemical proxies and their interpretation. YH, YS and MO contributed to stratigraphic correlation and interpretation of datasets. YH, YS and MO conducted geological surveys and sampling. All authors reviewed the submitted manuscript.

Authors' information

TI is a senior researcher of Geological Survey of Japan (GSJ), AIST, Japan; SU is a master's course student at Chiba University and an AIST research assistant, Japan; YH is a post-doc fellow at Geological

Survey of Japan (GSJ), AIST, Japan; KI is an assistant professor at Chiba University, Japan; YK is a researcher at the National Museum of Nature and Science, Japan; YS is an associate professor at NIPR, Japan; MO is a professor at Ibaraki University, Japan

Acknowledgements

We express our sincere gratitude to all members of the GSSP proposal for Chiba section samples. We are also grateful to Hitomi Yamazaki for assistance with conducting laboratory experiments.

References

Chinzei K, Fujioka K, Kitazato H, Koizumi I, Oba T, Oda M, Okada H, Sakai T, Tanimura Y (1987) Postglacial environmental change of the Pacific Ocean off the coasts of central Japan. Mar Micropaleontol 11(4):273–291.

Deser C, Alexander MA, Timlin MS (1999) Evidence for a wind-driven intensification of the Kuroshio Current Extension from the 1970s to the 1980s. J. Climate, 12, 1697-1706.

Elderfield H, Ferretti P, Greaves M, Crowhurst S, McCave IN, Hodell D, Piotrowski AM, 2012. Evolution of ocean temperature and ice volume through the mid-Pleistocene climate transition. Science 337: 704–709 http://dx.doi.org/10.1126/science.1221294.

Giaccio B, Regattieri E, Zanchetta G, Nomade S, Renne PR, Sprain CJ, Drysdale RN, Tzedakis PC, Messina P, Scardia G., Sposato A, Bassinot F (2015) Duration and dynamics of the best orbital analogue to the present interglacial. Geology 43: 603e606. https://doi.org/10.1130/G36677.1

GSSP Proposal Group (2019) A summary of the Chiba Section, Japan: a proposal of Global Boundary Stratotype Section and Point (GSSP) for the Middle Pleistocene Subseries. Jour Geol Soc Japan 125: 5-22.

Haneda Y, Okada M, Kubota Y, Suganuma Y (2020) Millennial-scale hydrographic changes in the northwestern Pacific during marine isotope stage 19: teleconnections with ice melt in the North Atlantic . Earth Planet Sci Lett 531, 115936. https://doi.org/10.1016/j.epsl.2019.115936

Hyodo M, Bradák B, Okada M, Katoh S, Kitaba I, Dettman DL, Hayashi H, Kumazawa K, Hirose K, Kazaoka O, Shikoku K, Kitamura A (2017) Millennial-scale northern Hemisphere Atlantic-Pacific climate teleconnections in the earliest Middle Pleistocene. Sci Rep 7: 10036. https://doi.org/10.1038/s41598-017-10552-2.

Hyodo, M., Kitaba, I. (2016) Timing of the MatuyamaeBrunhes geomagnetic reversal: Decoupled thermal maximum and sea-level highstand during Marine Isotope Stage 19. Quat Inter 383: 136–144. http://dx.doi.org/10.1016/j.quaint.2015.01.052.

Hyodo M, Katoh S, Kitamura A, Takasaki K, Matsushita H, Kitaba I, Tanaka I, Nara M, Matsuzaki M, Dettman DL, Okada M (2016) High resolution stratigraphy across the early-middle Pleistocene boundary from a core of the Kokumoto Formation at Tabuchi, Chiba Prefecture, Japan. Quat Inter 397: 16–26. https://doi.org/10.1016/j.quaint.2015.03.031.

Isono D, Yamamoto M, Irino T, Oba T, Murayama M , Nakamura T, Kawahata H (2009)The 1500-year climate oscillation in the midlatitude North Pacific during the Holocene Geology 37: 591–594, doi: 10.1130/G25667A

Itaki T (2009) Last glacial to Holocene polycystine radiolarians from the Japan Sea. News Osaka Micropaleontol (NOM) 14:43–89

Itaki T, Sagawa T, Kubota Y (2018) Data report: Pleistocene radiolarian biostratigraphy, IODP Expedition 346 Site U1427. In Tada, R., Murray, R.W., Alvarez Zarikian, C.A., and the Expedition 346 Scientists, Proceedings of the Integrated Ocean Drilling Program, 346: College Station, TX (Integrated Ocean Drilling Program). doi:10.2204/iodp.proc.346.202.2018

Izumi K, Haneda Y, Suganuma Y, Okada M, Kubota Y, Nishida N, Kawamata M, Matsuzaki T (submitted) Multiproxy geochemical analysis across the Lower–Middle Pleistocene boundary: Chemostratigraphy and palaeoenvironment of the Chiba composite section, central Japan. PEPS.

Kameo K, Kubota Y, Haneda Y, Suganuma Y, Okada M (submitted) Calcareous nannofossil biostratigraphy of the Lower–Middle Pleistocene boundary of the GSSP, Chiba composite section in the Kokumoto Formation, Kazusa Group, and implications for sea-surface environmental changes. PEPS.

Kazaoka O, Suganuma Y, Okada M, Kameo K, Head MJ, Yoshida T, Kameyama S, Nirei H, Aida N, Kumai H (2015) Stratigraphy of the Kazusa Group, Central Japan: a high-resolution marine sedimentary sequence from the Lower to Middle Pleistocene. Quat Int 383: 116-135.

Kleiven HF, Hall IR, McCave IN, Knorr G, Jansen E (2011) Coupled deep-water flow and climate variability in the Middle Pleistocene North Atlantic. Geology 39, 343–346. https://doi .org /10 .1130 /G31651.1

Koizumi I (2008) Diatom-derived SSTs (Td' ratio) indicate warm seas off Japan during the middle Holocene (8.2–3.3 kyr BP). Mar Micropal 69: 263–281.

Kuroyanagi A, Kawahata H, Nishi H, Honda M (2002) Seasonal changes in planktonic foraminifera in the northwestern North Pacific Ocean: sediment trap experiments from subarctic and subtropical gyres. Dee-Sea Res 49, 5627-5645. https://doi.org/10.1016/S0967-0645(02)00202-3

Matsuzaki KM, Itaki T (2017) New Northwest Pacific radiolarian data as a tool to estimate past sea surface and intermediate water temperatures. Paleoceanogr Paleoclimatol 32(3):218–245 https://doi.org/10.1002/ 2017PA003087

Minobe S (2002) Interannual to interdecadal changes of water temperature, sea-level displacement, and sea-ice distribution in the Bering Sea and associated atmospheric circulation changes. Prog Oceanogr 55: 45-64.

Motoyama I, Itaki T, Kamikuri S, Taketani Y, Okada M (2017) Cenozoic biostratigraphy, chronostratigraphy and paleoceanography in the Boso Peninsula and Bandai Volcano in the Aizu region, East Japan. Sci. Rep., Niigata Univ. (Geology), No. 32 (Supplement), 1–27.

Nigrini C (1970) Radiolarian assemblages in the North Pacific and their application to a study of Quarternary sediments in core V20–130, Geol. Soc. Am. Mem., 126, 39–175, doi:10.1130/MEM126-p139.

Nishibe Y, Takahashi K, Shiozaki T, Kakehi S, Saito H, Furuya K (2015) Size-fractionated primary production in the Kuroshio Extension and adjacent regions in spring. Journal Oceanography, 71: 27–40.

Nishida N, Kazaoka O, Izumi K, Suganuma Y, Okada M, Yoshida T, Ogitsu I, Nakazato H, Kameyama S, Kagawa A, Morisaki M, Nirei H (2016) Sedimentary processes and depositional environments of a continuous marine succession across the Lower-Middle Pleistocene boundary: Kokumoto Formation, Kazusa group, central Japan. Quat Int 397: 3-15

Nishikawa H, Usui N, Kamachi M1, Tanaka Y and Ishikawa Y (2016) Link between the interannual variability in the Kuroshio-Oyashio layered structure and the chlorophyll-a concentrations in the Kuroshio Extension during spring. Oceanography in Japan 25(5), 133-144 (in Japanese with English abstract).

Okada M, Suganuma Y, Haneda Y, Kazaoka O (2017) Paleomagnetic direction and paleointensity variations during the Matuyama-Brunhes polarity transition from a marine succession in the Chiba composite section of the Boso Peninsula, central Japan. Earth, Planets, Space 69 (45). https://doi.org/10.1186/s40623-017-0627-1.

Regattieri E, Giaccio B, Mannella G, Zanchetta G, Nomade S, Tognarelli A, Per-chiazzi N, Vogel H, Boschi C, Drysdale RN, Wagner B, Gemelli M, Tzedakis P (2019) Frequency and dynamics of millennial-scale variability during Marine Isotope Stage 19: insights from the Sulmona Basin (central Italy). Quat. Sci. Rev.214, 28–43. https://doi .org /10 .1016 /j .quascirev.2019 .04 .024.

Sánchez Goñi MF, Rodrigues T, Hodell DA, Polanco-Martínez JM, Alonso-García M, Hernández-Almeida I, Desprat S, Ferretti P (2016). Tropically-driven cli-mate shifts in southwestern Europe during MIS19, a low eccentricity inter-glacial. Earth Planet. Sci. Lett.448: 81–93. https://doi .org /10 .1016 /j .epsl .2016 .05 .018

Simon Q, Suganuma Y, Okada M, Haneda Y, ASTER team (2019) High-resolution 10Be and paleomagnetic recording of the last polarity reversal in the Chiba composite section: Age and dynamics of the Matuyama–Brunhes transition. Earth Planet Sci Lett 519: 92–100. https://doi.org/10.1016/j.epsl.2019.05.004.

Suganuma Y, Haneda Y, Kameo K, Kubota Y, Hayashi H, Itaki T, Okuda M, Head MJ, Sugaya M, Nakzato H, Igarashi A, Shikoku K, Hongo M, Watanabe M, Satoguchi Y, Takeshita Y, Nishida N, Izumi K, Kawamura K, Kawamata M, Okuno J, Yoshida T, Ogitsu I, Yabusaki H, Okada M (2018) Paleoclimatic and Paleoceanographic records of Marine Isotope Stage 19 at the Chiba composite section, central Japan: A reference for the Early-Middle Pleisotocene boundary. Quat Sci Rev 191: 406–430. https://doi.org/10.1016/j.quascirev.2018.04.022.

Suganuma Y, Okada M, Horie K, Kaiden H, Takehara M, Senda R, Kimura J, Haneda Y, Kawamura K, Kazaoka O, Head MJ (2015) Age of Matuyama-Brunhes boundary constrained by U-Pb zircon dating of a widespread tephra. Geology 43: 491-494

Tanaka I, Hyodo M, Kitaba I, Ueno U, Sato H (2017) Diatom-based paleoceanographic variability across the Early-Middle Pleistocene transition from the Chiba section, central Japan. Quat Int 455: 141-148

Yasudomi Y, Motoyama I, Oba T, Anma R (2014) Environmental fluctuations in the northwestern Pacific Ocean during the last interglacial period: evidence from radiolarian assemblages. Mar Micropaleontol 108:1–12

Tzedakis PC, Channell JET, Hodell DA, Kleiven HF, Skinner LC (2012) Determining the natural length of the current interglacial. Nature Geoscience 5, 138e142. https://doi.org/10.1038/ngeo1358

Tompson DWJ, Wallace JM (1998) The Arctic oscillation signature in the wintertime geopotential height and temperature fields. Geophys Res Lett 25: 1297-1300.

Supplementary Materials

Supplementary Table 1 Occurrence list of radiolarians from the CbCS in this study.

Supplementary Table 2 Relative abundance (%) of radiolarian indicator, Tr values and estimated summer SST from the CbCS. Dataset was compiled for this study and 41 preliminary results (Suganuma et al., 2018). Because 3 samples (YN-07, YN-09, YN-05) reported by Suganuma et al. (2018) are stratigraphically overlapped with newly analyzed samples, they were excluded from the dataset.

Supplementary Figure 1 (Lithologic column). Lithologic column and sampling horizon of the CbCS, modified from Suganuma et al. (2018). Stratigraphic correlation between the Urajiro, Yanagawa, Yoro River, Yoro-Tabuchi, and Kokusabata based on lithology and tephra beds are indicated by black dashed and red solid lines. The red solid lines especially indicate correlation points for reconstructing the age model of the TB-2 core (Supplementary Figure 4).

Supplementary Figure 2 Relative abundance changes of radiolarian species and species groups used for estimation of Tr value from compiled dataset of this study and Suganuma et al. (2018).

Supplementary Figure 3 Temporal profile of low field magnetic susceptibility and Ca/Ti. Black solid lines and circles are data from the CbCS (Okada et al., 2017; Simon et al., 2019; Izumi et al., under review). Light blue lines are data from the TB-2 core (Hyodo et al., 2016; 2017), which was dated using the latest age model of the CbCS by Suganuma et al. (2018). The age model of the TB-2 core, which was drilled at ~200 m northeast from the Chiba section (Hyodo et al. 2016), was obtained by tuning the diatom assemblage record from Osaka Bay (Hyodo and Kitaba 2015; Hyodo et al., 2017), whereas the chronology of the CbCS is based on tuning the benthic foraminifera oxygen isotope record to an astronomically dated sea level record from ODP 1123 (Elderfield et al., 2012; Suganuma et al., 2018). The difference of chronology hinders comparisons of paleoenvironmental records between the CbCS and TB-2 core. To resolve this issue, we converted the depth scale of the TB-2 core to the age scale of the CbCS using the latest age model by Suganuma et al. (2018) based on correlating six tephra beds and one upper limit of the mud crust bed (S. Fig. 1). Resultant temporal profiles of Ca/Ti ratio and low-field magnetic susceptibility of the TB-2 core show excellently synchronized variation with those of the CbCS (this S. Fig.; Hyodo et al., 2016; 2017; Okada et al., 2017; Simon et al., 2019; Izumi et al., under review). This indicates that the tephrostratigraphic and lithologic correlation allow us to compare the paleoenvironmental records between the CbCS and TB-2 core.

Figures

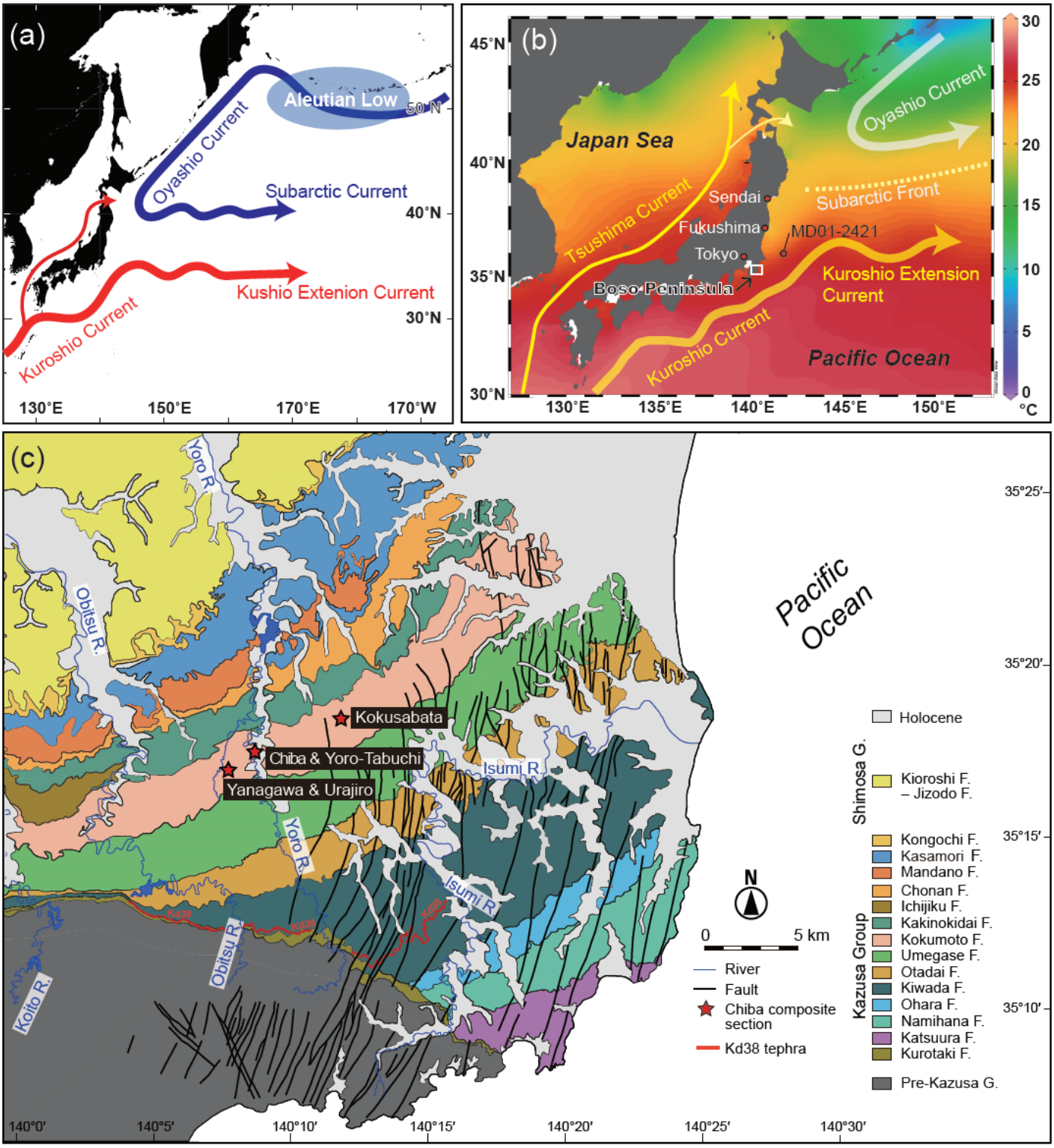

Figure 1

Maps showing (a) major ocean currents around Japan, (b) summer sea-surface temperature with location of Boso Peninsula, and (c) simplified geological map (Kazaoka et al., 2015). Red stars in (c) indicate locations of the Urajiro, Yanagawa, Yoro River, Yoro-Tabuchi, and Kokusabata sections that comprise the Chiba composite section (CbCS).

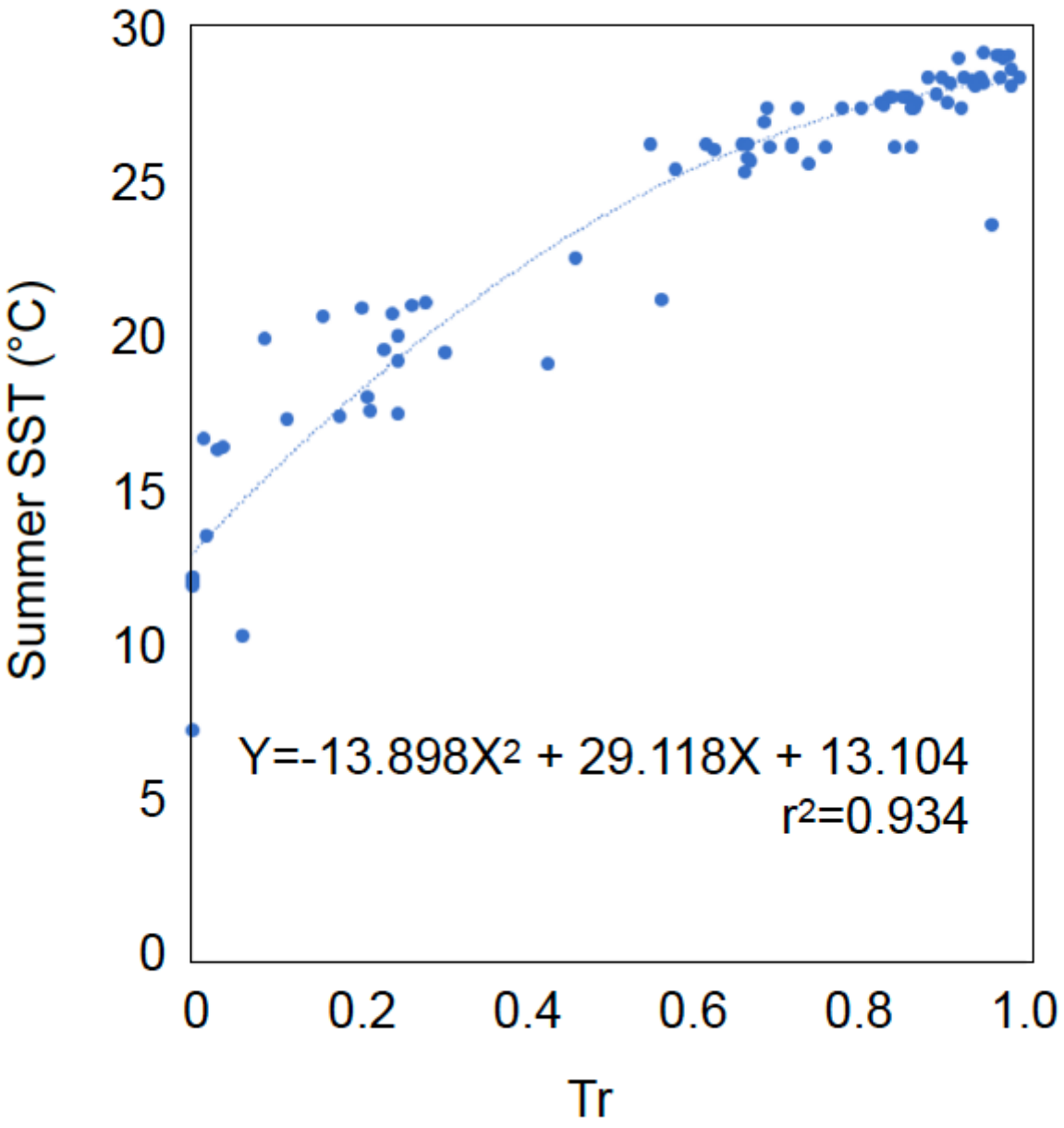

Figure 2

Plot showing the relationship between summer SST and Tr in the northwestern Pacific based on the dataset from Matsuzaki and Itaki (2017).

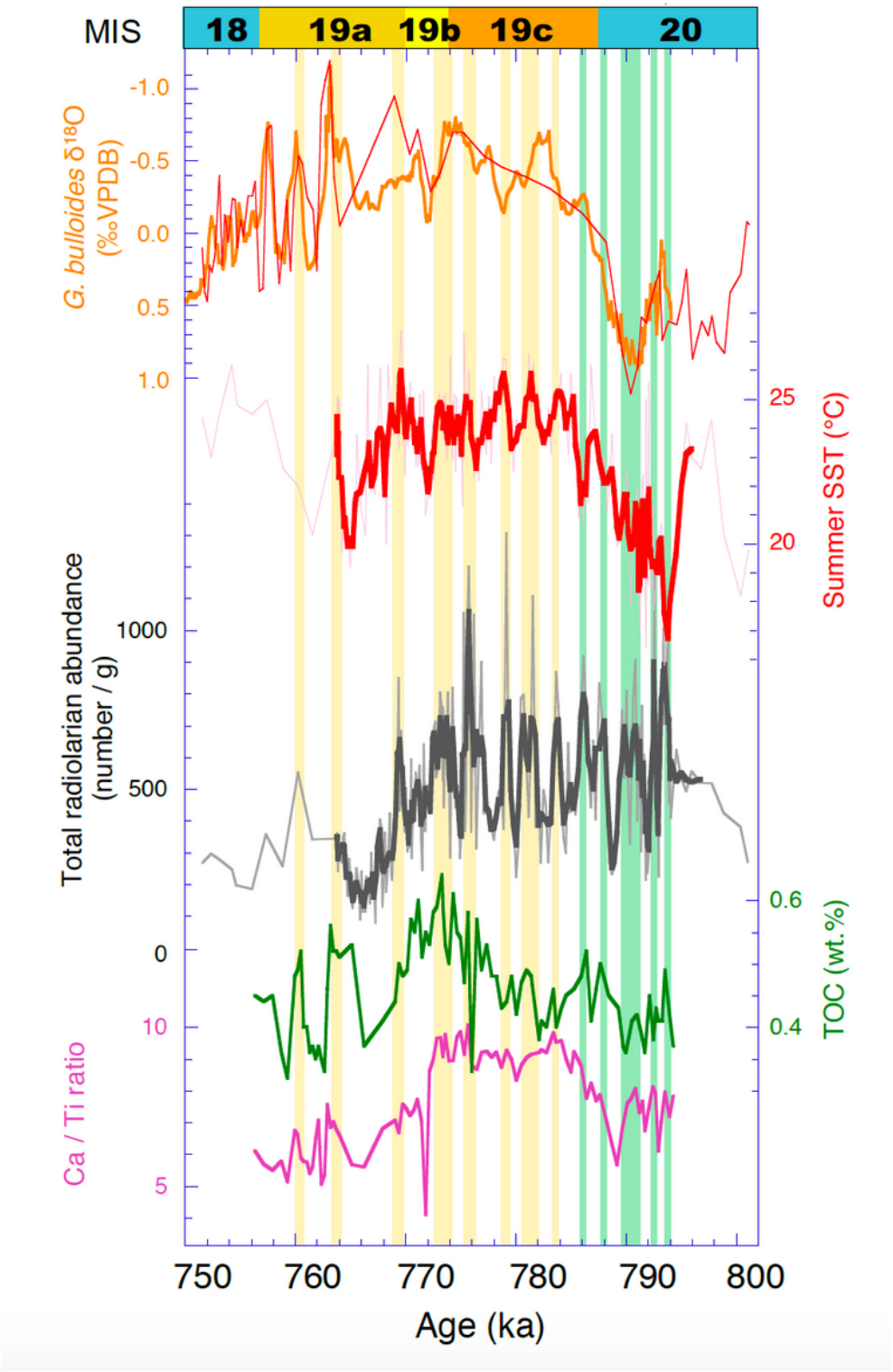

Figure 3

Comparisons among paleoceanographic the following proxies: (on the left y-axis) Oxygen isotope record of planktonic foraminifera Globigerina bulloides (heavy orange line indicates moving average over 5 points), total radiolarian abundance (heavy black line indicates moving average over 5 points) and Ca/Ti ratio (heavy magenta line) and (on the right y-axis) Tr-based summer SST (dots with thin line for original data and heavy red line indicating moving average for 3 points) and total organic carbon (TOC) (heavy

green line). Oxygen isotope records are from Haneda et al. (2020). TOC and Ca/Ti are from Izumi et al. (submitted). Pale yellow and green bands indicate intervals of radiolarian abundance maxima during warmer and colder periods, respectively.

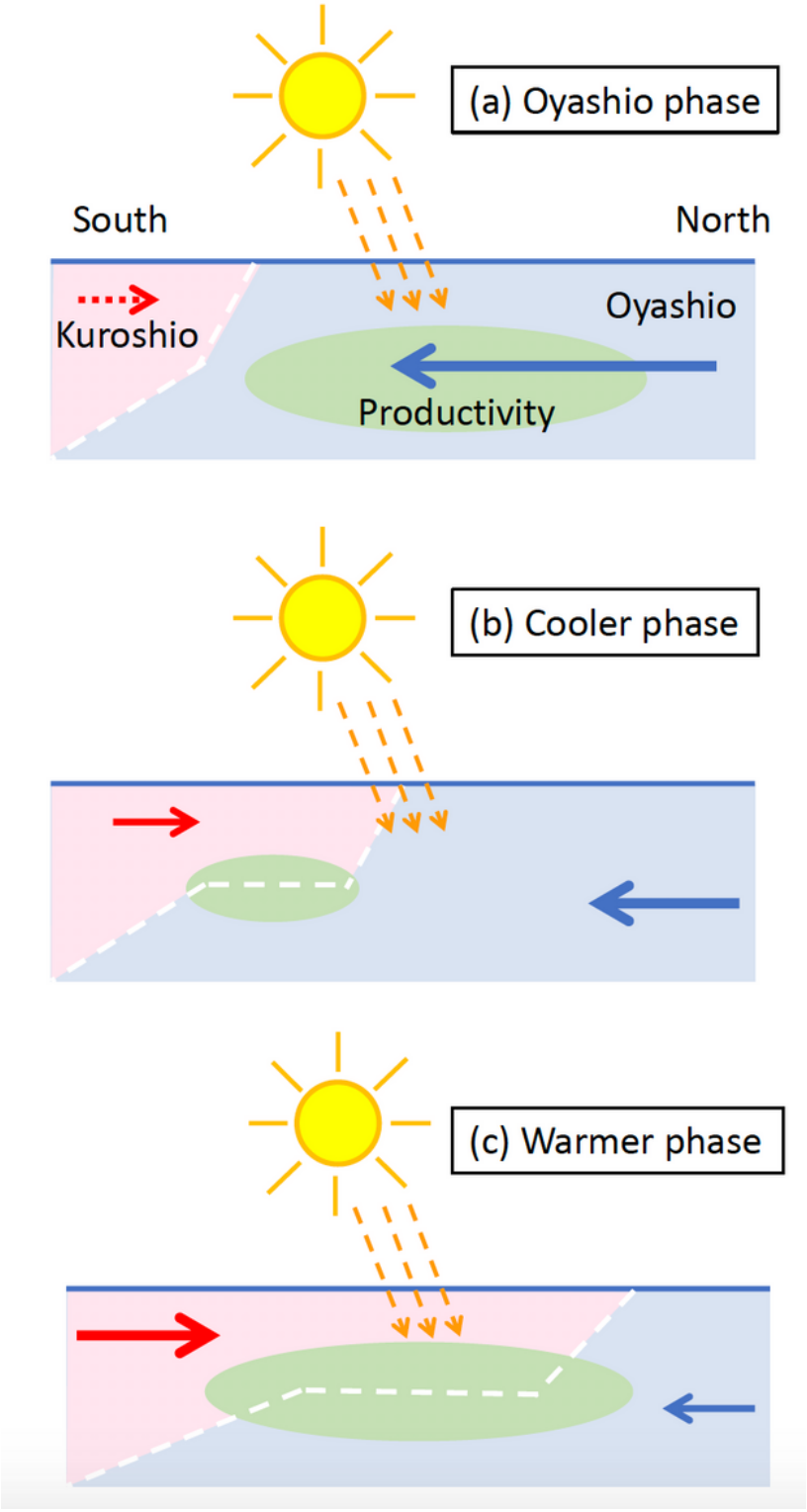

Figure 4

Schematics of oceanographic conditions indicating (a) Oyashio phase likely present in late MIS-20 characterized by high productivity and low temperature, and (b) cooler phase in MIS-19 when the

Kuroshio-Oyashio layered structure was contracted and (c) same conditions but with warmer phase with expanded layer structure.

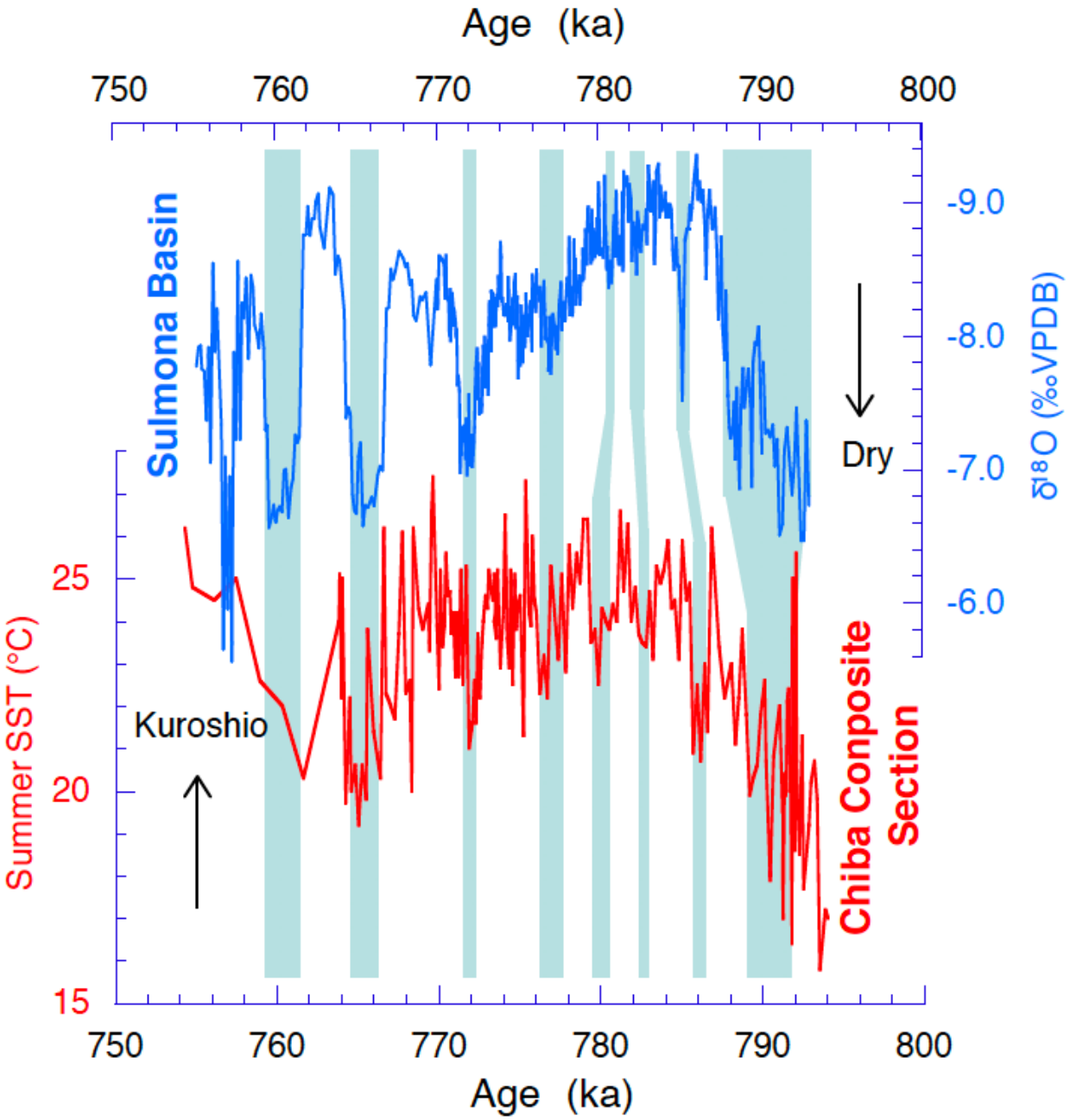

Figure 5

Probable correlations of paleo climate records between Sulmona Basin in Italy (Giaccio et al., 2015; Regattieri et al., 2019) and the CbCS in Japan (this study).

Supplementary Files

This is a list of supplementary files associated with this preprint. Click to download.

- SupplementTable2200422.xlsx
- SFig2200422.pdf
- SFig3191018.pdf
- GraphicAbst200422.pdf
- SupplementTable1200422.xlsx
- SFig1200422.pdf